

Spherical Porphyrin Sensor Array Based on Encoded Colloidal Crystal Beads for VOC Vapor Detection

Hua Xu,^{†,‡} Kai-Di Cao,[†] Hai-Bo Ding,[†] Qi-Feng Zhong,[†] Hong-Cheng Gu,[†] Zhuo-Ying Xie,[†] Yuan-Jin Zhao,[†] and Zhong-Ze Gu^{*,†,‡}

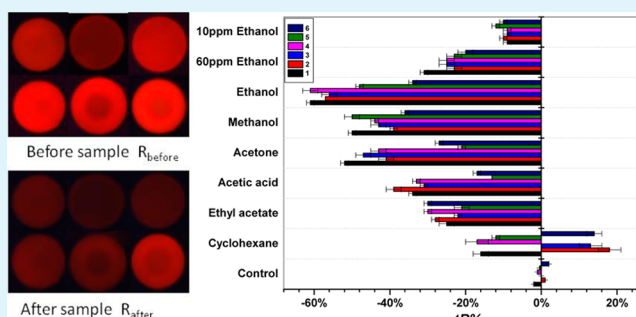
[†]State Key Laboratory of Bioelectronics, School of Biological Science and Medical Engineering, Southeast University, Si Pai Lou 2, Nanjing 210096, China

[‡]Suzhou Key Laboratory of Environment and Biosafety, Research Institute of Southeast University in Suzhou, Suzhou 215123, China

S Supporting Information

ABSTRACT: A spherical porphyrin sensor array using colloidal crystal beads (CCBs) as the encoding microcarriers has been developed for VOC vapor detection. Six different porphyrins were coated onto the CCBs with distinctive encoded reflection peaks via physical adsorption and the sensor array was fabricated by placing the prepared porphyrin-modified CCBs together. The change in fluorescence color of the porphyrin-modified CCBs array serves as the detection signal for discriminating between different VOC vapors and the reflection peak of the CCBs serves as the encoding signal to distinguish between different sensors. It was demonstrated that the VOC vapors detection using the prepared sensor array showed excellent discrimination: not only could the compounds from the different chemical classes be easily differentiated (e.g., alcohol vs acids vs ketones) but similar compounds from the same chemical family (e.g., methanol vs ethanol) and the same compound with different concentration ((e.g., Sat. ethanol vs 60 ppm ethanol vs 10 ppm ethanol) could also be distinguished. The detection reproducibility and the humidity effect were also investigated. The present spherical sensor array, with its simple preparation, rapid response, high sensitivity, reproducibility, and humidity insensitivity, and especially with stable and high-throughput encoding, is promising for real applications in artificial olfactory systems.

KEYWORDS: spherical sensor array, colloidal crystal, porphyrin, fluorescence color, encoded reflection peaks, VOC vapors detection



INTRODUCTION

The development of a rapid, low-cost gas identification system with a high sensitivity is in high demand for many applications, such as environmental monitoring, medical diagnosis, food quality control, and homeland security. In nature, mammals use about four hundred receptors to detect and discriminate between tens of thousands of different odorants.¹ Inspired by the mammalian olfactory system, an array-based sensing technology that utilizes multiple sensors, each having a partial specificity, that work in tandem to produce a unique composite response for each analyte, has emerged as a powerful new approach toward gas detection.^{2–5} Many arrays based on the modulation of electrical and gravimetric properties have been developed, and are used as artificial noses, also known as “electronic noses”. Although successfully commercialized, electronic noses generally suffer from being complex and expensive. Recently, artificial noses based on the modulation of optical signals, known as “photonic noses”, have emerged as a new player in this area, and these have the potential to be a simple, effective, low-cost, environmentally friendly, and portable sensor. Optical arrays based on a dye’s color,^{6–11} fluorescence,^{12–18} a photonic crystal’s color,¹⁹ and a hollow

photonic fiber’s infrared absorption²⁰ transducing signal have been developed.

The intensive study of biological olfactory systems shows that mammals may use metalloproteins as receptors to discriminate between different vapors.^{21–23} Because they have the same recognition mechanism as metalloproteins, porphyrins or metalloporphyrin dyes as sensing materials for photonic nose arrays has become a hot topic in the research in this field. A number of porphyrin sensor arrays have been fabricated to mimic mammalian olfactory systems for gas discrimination.^{6–11} In general, these arrays have mostly been fabricated by using a film as the substrate and spotting different porphyrin molecules at different positions. Although this method has the advantages of enabling a large sensor element capacity, the fabrication process is tedious and the arrays between different batches are discrete.

Recently, an alternative approach was proposed to fabricate the sensor elements using a homogeneous solution containing

Received: September 12, 2012

Accepted: November 19, 2012

Published: November 19, 2012

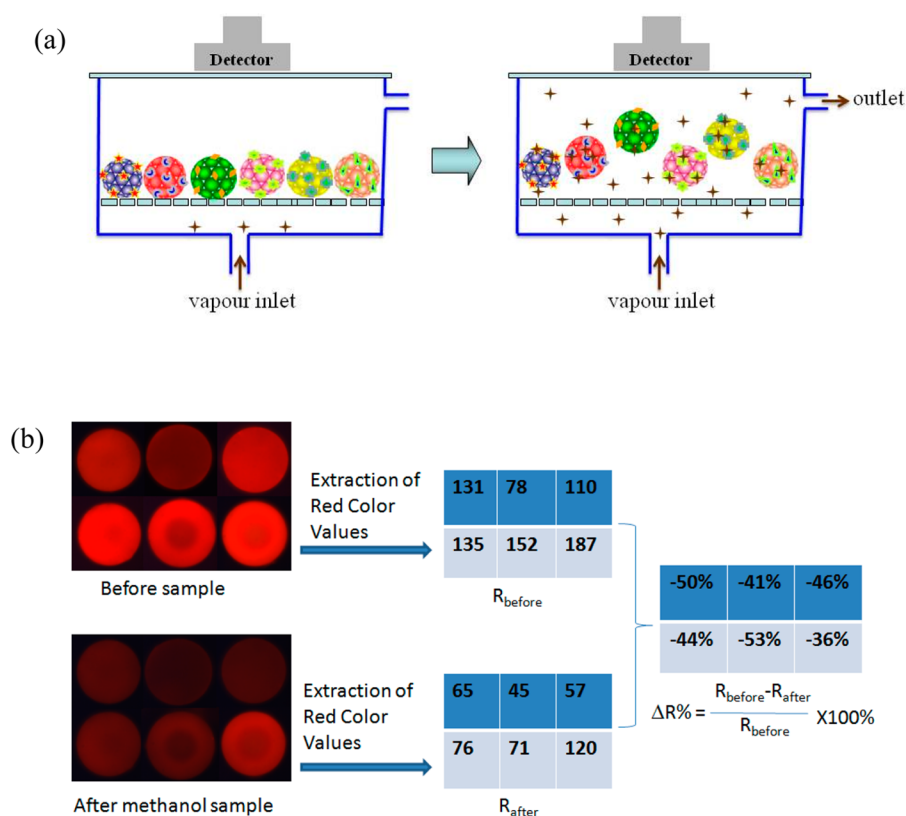


Figure 1. (a) Schematic diagram of the spherical gas sensor array composed of six porphyrin-modified CCBs to detect VOC vapors. The reflection peak of the CCBs was used to distinguish different sensors. (b) Schematic illustration of the basic steps in the fluorescence color imagery analysis to methanol in saturated atmosphere in the porphyrin-modified CCBs array. R_{before} and R_{after} denote the fluorescence red color value of the CCBs before and after exposure to VOC vapor, respectively.

bead carriers.^{12–18} In this method, billions of identically responding sensors can be fabricated simultaneously, and arrays have been produced by simple combining different sensor elements. Because each array is fabricated using only a small amount of the sensors, this procedure can be used to fabricate thousands of arrays that respond identically. However, a critical issue in this approach is that the sensors in the array are formed in a chaotic manner, and it is necessary to encode each bead to identify the different sensors.

One well-used encoding element is the fluorescence from dyes, which is also used as the detection signal for the vapor. This strategy requires the dye to have a different fluorescence for coding, and limits the use of different porphyrin dyes having a similar fluorescence in such bead-based arrays, even though they have been demonstrated to have excellent sensing performance in film-based arrays. The restriction on the number of dyes markedly affects the number of sensor units that can be fabricated, and more sensor units in an array usually mean that a higher accuracy can be achieved. Furthermore, a dye's fluorescence is very active in the vapor state, which can be a source of instability as an encoding element in long-term use. Therefore, a stable encoding approach that can be distinguished from the detection signal is anticipated.

In this paper, we propose the use of colloidal crystal beads (CCBs) as an encoding carrier to fabricate spherical porphyrin sensor arrays for volatile organic compound (VOC) vapor detection (Figure 1a). Six different porphyrins were coated onto the CCBs with different reflection peaks and the as-prepared porphyrin-modified CCBs were placed together as a sensor array. The change in fluorescence color of the CCB

array “before” and “after” exposure to the vapor serves as the detection signal for discriminating between different VOC vapors (Figure 1b), and the reflection peak of the CCBs serves as the encoding signal to distinguish between different sensors. As the reflection spectra originate from the physical nanostructure, determined by the diameter of the colloidal nanoparticles, the code is very stable and easily adjustable to incorporate a large encoding capacity.^{24–32} Different VOC vapors detection using the as-prepared sensor array showed excellent discrimination. The humidity effect, the detection reproducibility, the detection sensitivity and the reusability of the as-prepared porphyrin-modified sensor array were further investigated.

EXPERIMENTAL SECTION

Reagents and Instruments. *meso*-Tetraphenyl porphyrin (TPP), *meso*-tetra(4-carboxyphenyl)porphine tetramethyl ester (TCPP), 5-(4-aminophenyl)-10,15,20-triphenylporphyrin (TAPP), and metalloporphyrin complexes (ZnTPP, SnTPP, ZnTAPP) were prepared according to procedures outlined in the literature.^{33,34} Monodispersed silica nanoparticles were synthesized according to a modified Stöber method.³⁵ In this study, the VOC vapor samples were prepared from reagent-grade VOC liquid by a bubbling method and the experimental apparatus used for the preparation of VOC vapor were homemade according to literature (see Figure S1 in the Supporting Information).^{36,37} All measurements were performed at a constant temperature of 298 K and the saturated vapor pressures were calculated by Antoine's law. The saturated vapor was diluted with a N_2 stream to a controlled gas concentration for exposure testing. The gas flow rate was controlled by mass flow controllers (MFC) (Brooks 5850E) regulated and driven by a controller-unit (Beijing Sevenstar

Electronics, D08–4F). Different humidity was generated by different saturated salt solution.³⁸ SEM images were obtained using a scanning electron microscope (SEM, Hitachi S-3000N). The CCBs were observed using an optical microscope (Olympus BX-51) and images were recorded using a charge coupled device (CCD) (MediaCybernetics Evolution MP 5.0 RTV). Fluorescence images were captured using a fluorescence microscope (Olympus IX71). Fluorescence spectra of the CCBs were recorded using an optical microscope equipped with a fiber optic spectrometer (Ocean Optics, USB2000-FLG).

Preparation of Porphyrin-Modified CCBs. CCBs were fabricated by assembling monodisperse silica nanoparticles using a fluid device³¹ and calcined at 1000 °C for 3 h to improve the mechanical stability. Then, the CCBs were immersed in an acetone solution of trimethoxy(octadecyl)silane overnight. After being washed with acetone and dried, the CCBs were immersed in a chloroform solution of the desired porphyrin (1 mg/mL) overnight. Finally, the CCBs were washed with chloroform to remove excess porphyrin and dried in the dark at room temperature.

VOC Vapor Detection. The sensor array was placed in a 25 mL test chamber with an inlet, an outlet, and a transparent glass cover on the top and bottom surface respectively (see Figure S1 in the Supporting Information). The vapors were led continuous into the chamber and the test chamber was placed on the stage of fluorescence microscope to obtain the fluorescence color images of the CCB online. First, the reflection spectra of the CCBs were recorded and the fluorescence image of the porphyrin-modified CCBs array were obtained as the “before” fluorescence image. After exposure to the VOC vapor to equilibrium, the “after” fluorescence image were acquired. After this measurement, the reflection spectra of the CCBs were recorded to encode the different porphyrin-modified CCBs. Difference RGB value were obtained by taking the difference of the red values from each porphyrin-modified CCB from the “before” and “after” fluorescence images. As the color of the fluorescence of porphyrin is red, the color difference data of the porphyrin-modified beads were mostly concentrated in the R values of the RGB spectrum. The extraction of red color value and the subtractions were performed using the Matlab R2009a software package. HCA on the difference vectors was carried out using the Statistical Program for Social Science 13 software package. 3-Fold cross validation analysis was performed using the Matlab R2009a software.

RESULTS AND DISCUSSION

Fabrication and Characterization. The size-controlled CCBs microcarriers were fabricated by assembling monodisperse silica nanoparticles using a microfluidic device,²⁶ and their size was about 300 μm . By changing the diameter of the silica nanoparticles, six CCBs with different reflection peaks were obtained and used as microcarriers for the sensor array. The different reflection peaks were derived for encoding. Six porphyrins with different metal or different substituents (ZnTPP, SnTPP, *p*-NH₂ZnTPP, TPP, TCPP, and *p*-NH₂TPP) were chosen as sensing materials for the sensor array to achieve different selectivities and specificities (see Figure S2 in the Supporting Information). The CCBs were first treated with trimethoxy(octadecyl)silane to improve the surface hydrophobicity to achieve a uniform absorption on the porphyrin, and then the hydrophobic porphyrin was coated onto the CCBs via physical adsorption. The CCBs with different reflection peaks were modified with different porphyrins. Six types of different porphyrin-modified CCBs were placed together as a sensor array. In this way, array fabrication was simple, fast, and inexpensive, without the need for micromachining or other sophisticated means of micro-fabrication. However, the array obtained was random, in that the individual sensors were indiscriminate. Therefore, each

bead must be coded to discriminate between the different sensors.

Figure 2 shows the reflection spectra of the six CCBs and their porphyrin-modified CCBs. It can be seen that all the

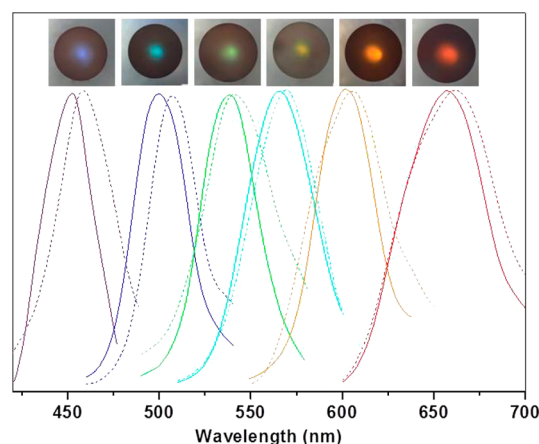


Figure 2. Reflection spectra of six CCBs (solid lines) and their porphyrin-modified CCBs (dotted lines). The insert shows six microscopic images of porphyrin-modified CCBs. The porphyrins used were: ZnTPP, SnTPP, ZnTAPP, TCPP, TAPP, and TPP. Measurements were performed in air.

beads exhibited unique reflection peaks, which can serve to differentiate one CCB sensor from another. On comparing the CCBs, the reflection spectra of their porphyrin-modified CCBs all showed shifts of several nanometers to longer wavelengths. This is because when the porphyrin was introduced onto the surface of the CCBs, it resulted in an increase in the refractive index, and according to Bragg's law, this leads to an increase in the peak wavelength. This result also indicates that the porphyrin was introduced onto the surface of the CCBs. Furthermore, the different porphyrin-modified CCBs sensors can easily be distinguished with the naked eye by observing microscopic images of the porphyrin-modified CCBs, which show an obvious different color in their center (see inset of Figure 2). The fluorescence microscopic images of porphyrin-modified CCBs shown in Figure 1b show a distinct red color, which is ascribed to the fluorescence of porphyrin. The uniform fluorescence color also indicated that the porphyrins were homogeneously distributed on the CCBs. SEM observations showed that there was no damage to the original structure of the CCBs after coating them with the porphyrin, and that the porphyrin molecules on the bead surface were uniform (see Figure S3 in the Supporting Information). The porous structure of the CCBs provided a large surface-to-volume ratio and a large number of channels for rapid gas diffusion. Therefore, a high sensitivity and rapid response would be expected using the encoded CCBs as a carrier for gas analysis and detection.

VOC Vapors Detection. The sensing performance of individual porphyrin-modified CCB sensors was first investigated using their fluorescence spectra. As shown in Figure 3, the fluorescence intensity of the CCB sensors exhibited an obvious decrease due to an interaction between the porphyrin and the ethanol vapor, and the rate of decrease reached an equilibrium after a period of about 5 min (see inset Figure 3a). This result showed the rapid response of our CCB sensor. However, unlike the film-based sensor, the fluorescence detection of the CCB sensor was difficult to confine to the

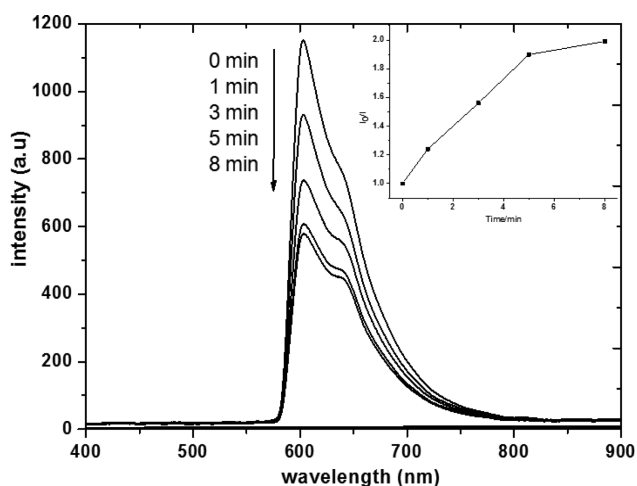


Figure 3. Fluorescence spectra of the ZnTPP-modified CCBs when exposed to ethanol vapor at 298 K ($\lambda_{\text{ex}} = 450$ nm). The inset shows a plot of I_0/I versus time, where I is the fluorescence intensity at 603 nm.

same place each time owing to movement and rotation, which often resulted in an inaccuracy in the detection because the fluorescence intensity in the different areas of the CCBs often showed small fluctuations. To solve this problem, we used the change in the fluorescence color of the entire porphyrin-modified CCBs as the response signal for vapor detection, as shown in Figure 1b.

To demonstrate the ability of the porphyrin-modified CCBs sensor array to discriminate between gas analytes, eight VOC vapors including alcohols, carboxylic acids, ketones, ester and alkanes, and a control experiment were tested for. Fluorescence images of every CCBs sensor are described by RGB color values. The different CCBs sensor was distinguished by the reflection spectra of the CCBs. As the color of the fluorescence of porphyrin is red, the color data of the porphyrin-modified beads were mostly concentrated in the R values of the RGB spectrum. Change in the fluorescence R value is generated by

taking the difference value of R values between the “before” and “after” exposure to VOC vapor (Figure 1b).

As shown in Figure 4, different changes in the fluorescence R values were obtained for the vapors for different CCB sensors, which functioned as a “fingerprint” for each vapor, and gave us intuitionistic information on the difference between the vapors. Using these results, a facile discrimination of one vapor from another could be achieved. Control experiment showed no obvious changes in the fluorescence R values of the CCB sensor array. These results also highlight the excellent ability of the CCB arrays to discriminate between common organic functional groups. The different changes in R values were ascribed to the different recognition ability of the porphyrins to VOC compounds. Strong molecular interactions are favorable for electron transfer between the porphyrin and VOC analyte, and resulted in an obvious change in fluorescence color value. As shown in Figure 4, three CCB sensors (1–3) used metalloporphyrin as sensing materials also exhibited larger R value change than those sensor based on free porphyrin with substituents (4–6). This result indicated that metal coordinated to porphyrin strongly influences the sensitivity of the resulting sensor. When the VOC molecular contains a donor atom, such as oxygen, the most important effect of the central metal can be directly related to the coordinative interactions between the VOC and the metal. Among three free porphyrin sensors, the sensor used the porphyrin bearing tetracarboxyl methyl ester as sensing materials exhibited large R value changes. This may be ascribed that the tetracarboxyl methyl ester substituents of porphyrin enhance nonspecific interaction with VOC. In the case of the cyclohexane, the coordination to the metal can be excluded and the mainly interaction is based on nonspecific absorption to porphyrin. Therefore, compared to other VOC vapor, the results of cyclohexane detection exhibited small R value changes.

Furthermore, not only could the compounds from the different chemical classes be easily differentiated (e.g., alcohol vs acids vs ketones), but similar compounds from the same chemical family (e.g., methanol vs ethanol) and the same compound with different concentration ((e.g., Sat. ethanol vs 60 ppm ethanol vs 10 ppm ethanol) could also be distinguished

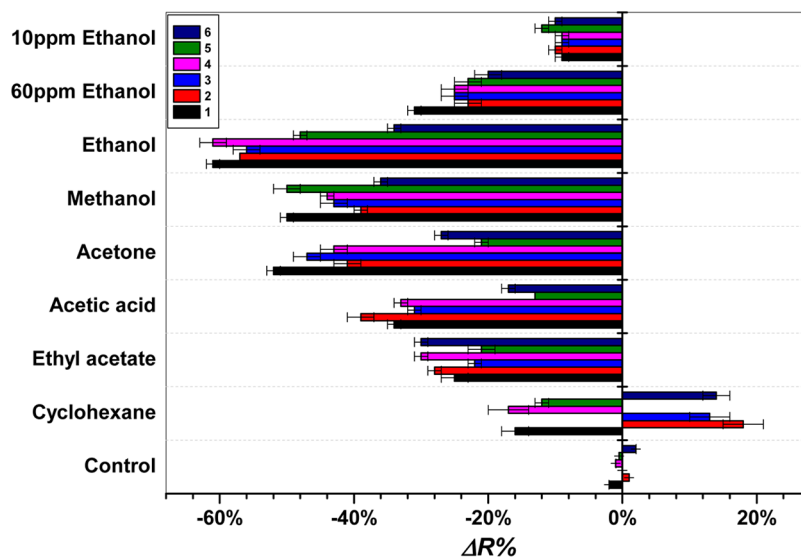


Figure 4. Response of a sensor array composed of six porphyrin-modified CCBs to VOCs vapor and a control experiment at 298K. Average of three trials is shown. The full digital data are provided in the Supporting Information, Table S2.

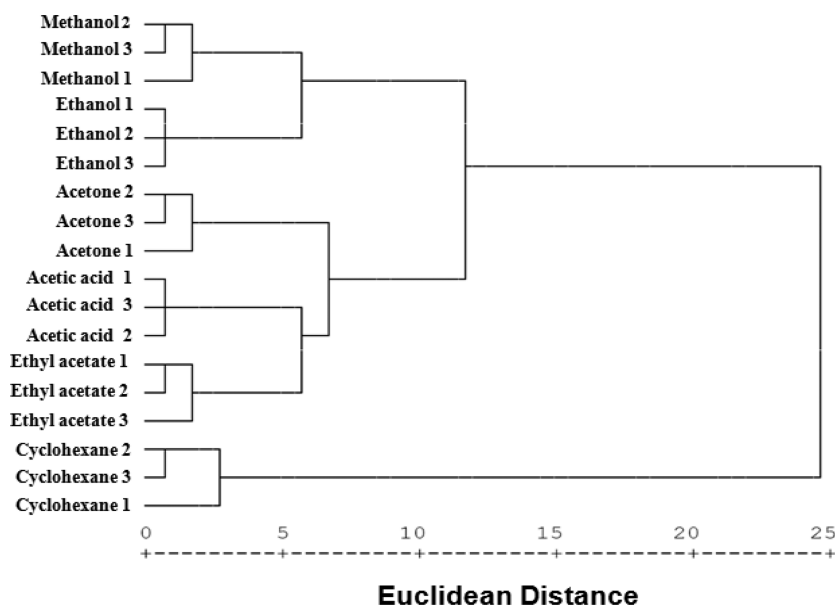


Figure 5. Hierarchical cluster analysis (HCA) for six VOC vapors at their saturated vapor pressure at 298 K. All of the experiments were run in triplicate and the HCA analysis uses all 18 individual trials;

using our sensor array, as they exhibited distinct differences in R color values (Figure 4). The above results show the high sensitivity of our CCB array in discriminating different VOC vapors. After each measurement, the used sensor array was left exposed to a nitrogen atmosphere to recover (see Figure S4 in the Supporting Information). In this way, the sensor array could be reused many times, which is important in developing low-cost artificial olfactory systems. It can be seen that 90% fluorescence color recovery of the used sensor need to about 30 min (see Figure S4b in the Supporting Information). This result also indicated that these vapor molecular probably develop significant interactions with porphyrin and the polymer matrix that must be overcome for the molecules to leave the material, which takes some time.

Reproducibility. Triplicate data were acquired by three independent experiments from three separate beads to probe the reproducibility of the array response to each VOC vapors. The high dispersion of the sensor array data was compared and classified by hierarchical cluster analysis (HCA) technique. The HCA technique is based on a grouping of the analyte vectors according to their spatial distances in their full vector space. The main purpose of the HCA technique is to divide the analytes into discrete groups based on the characteristics of their respective responses. The resulting dendrograms based on our array response data in Figure 5 showed the clusters formed are in keeping with the structural and electronic properties of the VOCs. In triplicate trials, all saturated vapors and the vapor with different concentration (see Figure S5 in the Supporting Information) were accurately identified with no error or misclassifications using our sensor array. This result indicated excellent reproducibility of our CCBs sensor array to VOC vapor.

To estimate generalization error of our CCBs sensor array, 3-fold cross validation was used to analyze the data set. First, the data set in Figure 5 is randomly divided into three subsets. Each time, one of three subsets is used as the test set and the other two subsets are put together to form a training set. Three subsets were alternately used as a test to repeat above process. Then the classification accuracy of three classifiers was obtained

and their average value was used as the performance index of the classifiers. As shown in Table S1 in the Supporting Information, 3-fold cross validation analysis of the data set showed a low average error rate, only 0.0741. This result also indicated that our sensor array have good prediction to unknown VOCs.

Humidity Insensitivity. The interference of atmospheric humidity on sensor performance is a serious problem with current electronic nose technology.³⁸ Because porphyrin of our array is hydrophobic, water-insoluble dye and coated onto hydrophobic CCBs, these arrays are essentially impervious to changes in relative humidity (RH). As shown in Figure 6, porphyrin-modified CCBs sensor array are essentially unresponsive to water vapor from saturated salt solutions whose water vapor pressures ranged from 11 to 97% RH.³⁹ Similarly, the response to other analytes is not affected by the presence of RH over this range.

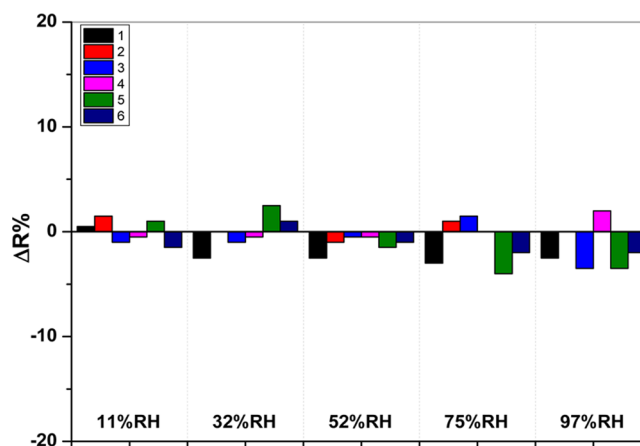


Figure 6. Porphyrin-modified CCBs sensor array is essentially unaffected by humidity over a wide range from 11% to 97% RH; average of two trials is shown. The full digital data are provided in the Supporting Information, Table S2.

Our CCB sensor have a hydrophobicity polymer matrix surface by treating with trimethoxy(octadecyl)silane and the porphyrin is dispersed in the polymer matrix. The different response of our sensor toward alcohols and water can be explained in terms of a different permeation capability of the analytes into the polymer matrix of the CCB surface. The larger alcohol solubility into the polymer can be ascribed to the presence of the aliphatic moiety in the alcohol molecular, which at the same time is able to interact with the less polar moieties such as long-chain alkane and benzene rings and with the metal portion of metalloporphyrin by metal-coordination bond. Similar results have been reported in recently published paper.^{7,40}

CONCLUSIONS

In summary, we have developed a spherical porphyrin sensor array using CCBs as the encoding microcarriers. VOC vapor detection by our CCB sensor array displayed excellent discrimination among a very wide range of compounds. The present spherical sensor array, with its simple preparation, rapid response, high sensitivity, reproducibility, and humidity insensitivity, and especially with stable and high-throughput encoding, is promising for real applications in artificial olfactory systems.

ASSOCIATED CONTENT

Supporting Information

Gas mixing rig, chemical structure of porphyrin, SEM image, reversibility study, and full digital data. This material is available free of charge via the Internet at <http://pubs.acs.org>.

AUTHOR INFORMATION

Corresponding Author

*E-mail: gu@seu.edu.cn.

Notes

The authors declare no competing financial interest.

ACKNOWLEDGMENTS

This work was supported by the NSFC (Grants 21103020, 51102043, and 50925309), the Suzhou Science and Technology Department (Grants SYG201209, SH201110), the National Basic Research Program of China (Grants 2012CB933302).

REFERENCES

- (1) Persaud, K.; Dodd, G. *Nature* **1982**, *299*, 352–355.
- (2) Albert, K. J.; Lewis, N. S.; Schauer, C. L.; Sotzing, G. A.; Stitzel, S. E.; Vaid, T. P.; Walt, D. R. *Chem. Rev.* **2000**, *100*, 2592–2626.
- (3) Diamond, D. *Electroanal.* **1993**, *5*, 795–802.
- (4) Bourgeois, W.; Romain, A. C.; Nicolas, J.; Stuetz, R. M. *J. Environ. Monitor.* **2003**, *42*, 852–860.
- (5) Ding, L.; Du, D.; Zhang, X. J.; Ju, H. X. *Curr. Med. Chem.* **2008**, *15*, 3160–3170.
- (6) Rakow, N. A.; Suslick, K. S. *Nature* **2000**, *406*, 710–714.
- (7) Janzen, M. C.; Ponder, J. B.; Bailey, D. P.; Ingison, C. K.; Suslick, K. S. *Anal. Chem.* **2006**, *78*, 3591–3600.
- (8) Sen, A.; Albarella, J. D.; Carey, J. R.; Kim, P.; McNamara, W. B., III. *Sens. Actuators, B* **2008**, *134*, 234–237.
- (9) Paolesse, R.; Lvova, L.; Nardis, S.; Natale, C. D.; D'Amico, A. F.; Castro, L. *Microchim. Acta* **2008**, *163*, 103–112.
- (10) Lim, S. H.; Kemling, J. W.; Feng, L.; Suslick, K. S. *Analyst* **2009**, *134*, 2453–2457.
- (11) Bang, J. H.; Lim, S. H.; Park, E.; Suslick, K. S. *Langmuir* **2008**, *24*, 13168–13172.
- (12) Dickinson, T. A.; Michael, K. L.; Kauer, J. S.; Walt, D. R. *Anal. Chem.* **1999**, *71*, 2192–2198.
- (13) Bencic-Nagale, S.; Walt, D. R. *Anal. Chem.* **2005**, *77*, 6155–6162.
- (14) Walt, D. R. *Curr. Opin. Chem. Biol.* **2010**, *14*, 767–770.
- (15) Aernecke, M. S.; Walt, D. R. *Sens. Actuators, B* **2009**, *142*, 464–469.
- (16) Stitzel, S. E.; Cowen, L. J.; Albert, K. J.; Walt, D. R. *Anal. Chem.* **2001**, *73*, 5266–5271.
- (17) Bencic-Nagale, S.; Sternfeld, T.; Walt, D. R. *J. Am. Chem. Soc.* **2006**, *128*, 5041–5048.
- (18) Albert, K. J.; Gill, D. S.; Pearce, T. C.; Walt, D. R. *Anal. Bioanal. Chem.* **2002**, *373*, 792–802.
- (19) Bonifacio, L. D.; Puzzo, D. P.; Breslav, S.; Willey, B. M.; McGeer, A.; Ozin, G. A. *Adv. Mater.* **2010**, *22*, 1351–1354.
- (20) Yildirim, A.; Vural, M.; Yaman, M.; Bayindir, M. *Adv. Mater.* **2011**, *23*, 1263–1267.
- (21) Suslick, K. S. *MRS Bull.* **2004**, *29*, 720–725.
- (22) Natale, C. D.; Martinelli, E.; Paolesse, R.; D'Amico, A.; Filippini, D.; Lundström, I. *Plos One* **2008**, *3*, e3139.
- (23) Natale, C.; Di, Martinella, E.; Paolesse, R.; D'Amico, A.; Filippini, D.; Lundström, I. *Sens. Actuators, B* **2009**, *142*, 412–417.
- (24) Zhao, X. W.; Cao, Y.; Fuyumi, I.; Chen, H. H.; Nagai, K.; Zhao, Y. H.; Gu, Z. Z. *Angew. Chem., Int. Ed.* **2006**, *45*, 6835–6838.
- (25) Zhao, Y. J.; Zhao, X. W.; Gu, Z. Z. *Adv. Funct. Mater.* **2010**, *20*, 2970–2988.
- (26) Zhao, Y. J.; Zhao, X. W.; Sun, C.; Li, J.; Zhu, R.; Gu, Z. Z. *Anal. Chem.* **2008**, *80*, 1598–1605.
- (27) Li, J.; Zhao, X. W.; Zhao, Y. J.; Gu, Z. Z. *Chem. Commun.* **2009**, 2329–2331.
- (28) Li, J.; Zhao, X. W.; Zhao, Y. J.; Hu, J.; Xu, M.; Gu, Z. Z. *J. Mater. Chem.* **2009**, *19*, 6492–6497.
- (29) Zhao, Y. J.; Zhao, X. W.; Tang, B. C.; Xu, W. Y.; Gu, Z. Z. *Langmuir* **2008**, *26*, 6111–6114.
- (30) Xu, H.; Zhu, C.; Zhao, Y. J.; Zhao, X. W.; Hu, J.; Gu, Z. Z. *J. Nanosci. Nanotechnol.* **2009**, *9*, 2586–2591.
- (31) Zhao, Y. J.; Zhao, X. W.; Pei, X. P.; Hu, J.; Zhao, W. J.; Chen, B. A.; Gu, Z. Z. *Anal. Chim. Acta* **2009**, *633*, 103–108.
- (32) Sun, C.; Zhao, X. W.; Zhao, Y. J.; Zhu, R.; Gu, Z. Z. *Small* **2008**, *4*, 592–596.
- (33) Xu, H.; Zheng, J. Y. *Macromol. Chem. Phys.* **2010**, *211*, 2125–2131.
- (34) Xu, H.; Zhu, Y. Z.; Zheng, J. Y. *Supramol. Chem.* **2007**, *19*, 365–372.
- (35) Stober, W.; Fink, A.; Bohn, E. J. *Colloid Interface Sci.* **1968**, *26*, 62–69.
- (36) Penza, M.; Rossi, R.; Aivisi, M.; Signore, M. A.; Serra, E.; Paolesse, R.; D'Amico, A.; Di Natale, C. *Sens. Actuators, B* **2010**, *144*, 387–394.
- (37) Dunbar, A. D. F.; Richardson, T. H.; McNaughton, A. J.; Hutchinson, J.; Hunter, C. A. *J. Phys. Chem. B* **2006**, *110*, 16646–16651.
- (38) O'Brien, F. E. M. *J. Sci. Instrum.* **1948**, *25*, 73–76.
- (39) Konvalina, G.; Haick, H. *ACS Appl. Mater. Interfaces* **2012**, *1*, 317–325.
- (40) Carturana, S.; Tonezzer, M.; Quarantab, A.; Maggionia, G.; Buffab, M.; Milana, R. *Sens. Actuators, B* **2009**, *137*, 281–290.